Electronic Supplementary Material (ESI) for Inorganic Chemistry Frontiers.
This journal is © the Partner Organisations 2024

Electronic Supporting Information

Narrow-band Circularly Polarized Red Electroluminescence in Trinuclear Clusters

Xin Yang,[a,d] Han Cheng,[a,b,] Lin-Xi Shi,[a] Jin-Yun Wang,[a] and Zhong-Ning Chen[a,b,c,d,*]

[a] *State Key Laboratory of Structural Chemistry, Fujian Institute of Research on the Structure of Matter, Chinese Academy of Sciences, Fuzhou, Fujian 350002, China*. E-mail: czn@fjirsm.ac.cn

[b] *School of Physical Science and Technology, Shanghai Tech University, Shanghai 201210, China*

[c] *Fujian Science & Technology Innovation Laboratory for Optoelectronic Information of China, Fuzhou, Fujian 350108, China*

[d] *University of Chinese Academy of Sciences, Beijing, 100049, China*

Experimental Section

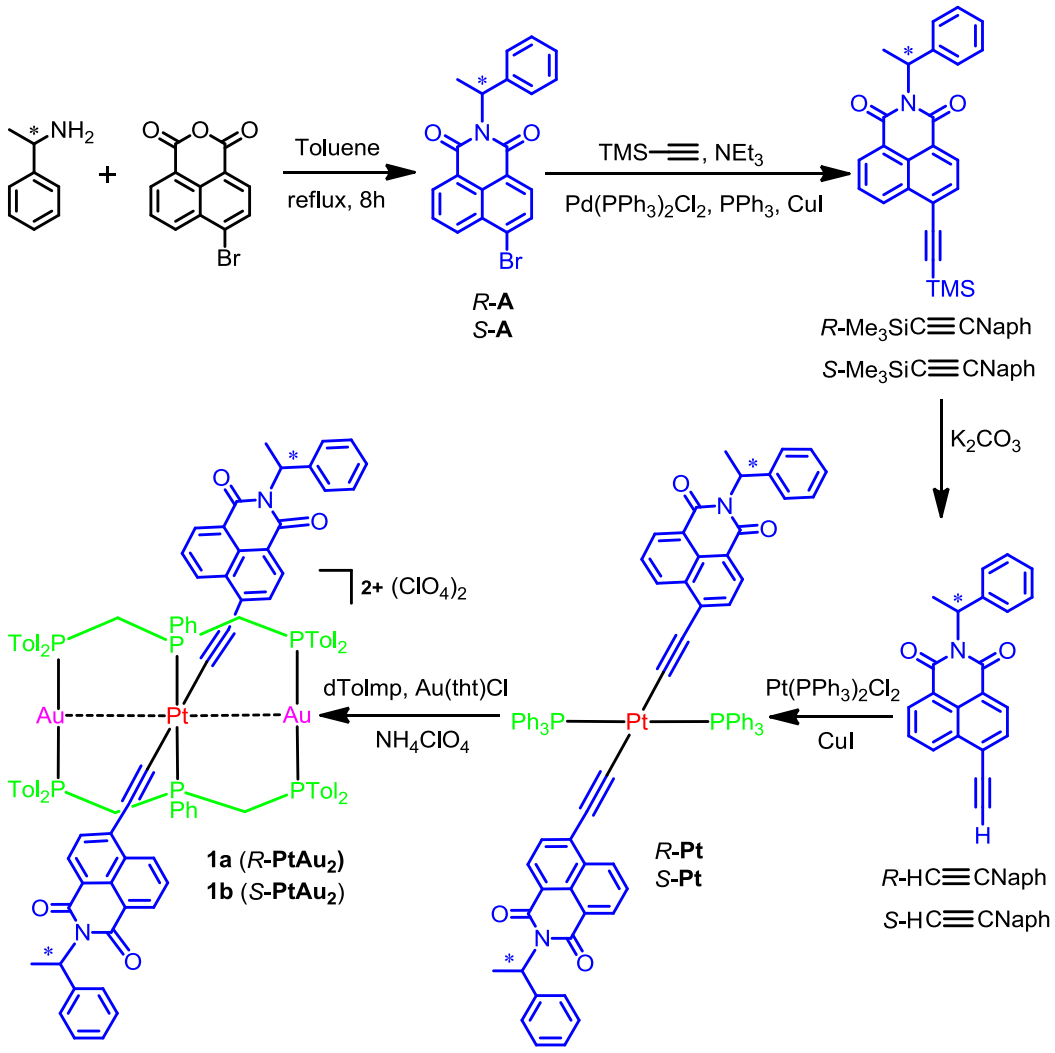

Scheme 1. Synthetic routes to *R*/*S*-$PtAu_2$ clusters.

Synthesis of 4-bromo-N-(1-phenylethyl)-1,8-naphthimide (A). Under argon atmosphere, 4-bromo-1,8-naphthalic anhydride (4.00 g, 14.4 mmol) and alpha-methylbenzylamine (2.2 mL, 17.3 mmol) were added to 100 mL toluene. After stirring at 110℃ for 12 h, the solution was cooled down to room temperature, evaporated and chromatographed on silica gel using dichloromethane/petroleum as eluent to get the yellow solid product. Yield: 64%.

***R*-A**. ^{1}H NMR (600 MHz, $CDCl_3$): δ 8.66 – 8.58 (m, 1H), 8.58 – 8.51 (m, 1H), 8.38 (ddd, *J* = 8.0, 3.3, 1.6 Hz, 1H), 8.04 – 8.00 (m, 1H), 7.86 – 7.79 (m, 1H), 7.52 – 7.48 (m, 2H), 7.32 (t, *J* = 7.6 Hz, 2H), 7.26 – 7.22 (m, 1H), 6.53 (q, *J* = 7.1 Hz, 1H), 1.99 (dd, *J* = 7.1, 1.7 Hz, 3H). ^{13}C NMR (151

MHz, chloroform-*d*): δ 163.95, 163.92, 140.84, 133.43, 132.50, 131.70, 131.38, 130.78, 130.43, 129.33, 128.48, 128.39, 127.47, 127.37, 123.67, 122.80, 50.58, 16.53.

***S*-A**. ^{1}H NMR (400 MHz, $CDCl_3$): δ 8.62 (dd, *J* = 7.3, 1.2 Hz, 1H), 8.56 (dd, *J* = 8.5, 1.1 Hz, 1H), 8.38 (d, *J* = 7.9 Hz, 1H), 8.03 (d, *J* = 7.9 Hz, 1H), 7.83 (dd, *J* = 8.5, 7.3 Hz, 1H), 7.53 – 7.45 (m, 2H), 7.32 (dd, *J* = 8.4, 6.8 Hz, 2H), 7.24 (t, *J* = 7.3 Hz, 1H), 6.53 (q, *J* = 7.1 Hz, 1H), 1.98 (d, *J* = 7.1 Hz, 3H). ^{13}C NMR (151 MHz, Chloroform-*d*): δ 163.96, 163.94, 140.85, 133.45, 132.52, 131.72, 131.40, 130.82, 130.45, 129.36, 128.48, 128.41, 127.47, 127.37, 123.70, 122.83, 50.59, 16.54.

Synthesis of 4-trimethylsilylethynyl-N-(1-phenylethyl)-1,8-naphthimide ($Me_3SiC{\equiv}CNaph$). Under argon atmosphere, to a NEt_3 solution of 4-bromo-N-(1-phenylethyl)-1,8-naphthimide (1 g, 2.63 mmol) were added $Pd(PPh_3)_2Cl_2$ (55 mg, 0.08 mmol)、PPh_3 (43 mg, 0.16 mmol), CuI (30 mg, 0.16 mmol) and trimethylsilylacetylene (0.75 mL, 5.26 mmol). After stirring at 90℃ for 8 h, the solution was cooled down to room temperature, which was evaporated and chromatographed on silica gel using dichloromethane-petroleum (v/v = 20 : 1) as eluent to get the yellow soild product. Yeild: 76%.

***R*-$Me_3SiC{\equiv}CNaph$**. ^{1}H NMR (600 MHz, $CDCl_3$): δ 8.65 – 8.55 (m, 2H), 8.52 – 8.44 (m, 1H), 7.87 (dd, *J* = 7.6, 1.4 Hz, 1H), 7.84 – 7.77 (m, 1H), 7.50 (ddt, *J* = 7.3, 2.1, 1.0 Hz, 2H), 7.32 (t, *J* = 7.8 Hz, 2H), 7.25 – 7.21 (m, 1H), 6.53 (q, *J* = 7.1 Hz, 1H), 1.98 (dd, *J* = 7.1, 0.8 Hz, 3H), 0.36 (d, *J* = 0.8 Hz, 9H). ^{13}C NMR (101 MHz, chloroform-*d*) δ 164.47, 164.19, 141.13, 132.78, 132.20, 132.15, 131.66, 130.87, 128.58, 128.46, 127.97, 127.62, 127.61, 127.42, 123.66, 123.06, 105.72, 101.70, 50.64, 16.69.

***S*-$Me_3SiC{\equiv}CNaph$**. ^{1}H NMR (400 MHz, $CDCl_3$) δ 8.66 – 8.55 (m, 2H), 8.48 (d, *J* = 7.7 Hz, 1H), 7.88 (d, *J* = 7.6 Hz, 1H), 7.82 – 7.77 (m, 1H), 7.50 (d, *J* = 7.5 Hz, 2H), 7.32 (t, *J* = 7.6 Hz, 2H), 7.23 (t, *J* = 7.3 Hz, 1H), 6.53 (q, *J* = 7.1 Hz, 1H), 1.98 (d, *J* = 7.1 Hz, 3H), 0.36 (s, 9H). ^{13}C NMR (151 MHz, chloroform-*d*): δ 164.37, 164.09, 141.02, 132.69, 132.11, 132.04, 131.56, 130.77, 128.48, 128.35, 127.87, 127.49, 127.32, 123.53, 122.94, 105.61, 101.58, 50.50, 16.56.

Synthesis of 4-ethynyl-N-(1-phenylethyl)-1,8-naphthimide ($HC{\equiv}CNaph$). Under argon atmosphere, $Me_3SiC{\equiv}CNaph$ (0.2 g, 0.5 mmol) and K_2CO_3 (0.34 g, 2.5 mmol) were added to 10 mL mixture solution of MeOH and CH_2Cl_2. After stirring at room temperature for 8 h away from light,

the reaction solution is filtered and extracted with EA and NaCl (aq) to get yellow solid product. Yield: 85%.

***R*-HC≡CNaph:** ^{1}H NMR (400 MHz, $CDCl_3$) δ 8.65 (ddd, *J* = 20.4, 7.9, 1.2 Hz, 2H), 8.52 (d, *J* = 7.6 Hz, 1H), 7.94 (d, *J* = 7.6 Hz, 1H), 7.83 (dd, *J* = 8.4, 7.3 Hz, 1H), 7.55 – 7.49 (m, 2H), 7.34 (dd, *J* = 8.4, 6.8 Hz, 2H), 7.25 (t, *J* = 7.3 Hz, 1H), 6.56 (q, *J* = 7.1 Hz, 1H), 3.75 (s, 1H), 2.01 (d, *J* = 7.1 Hz, 3H).

***S*-HC≡CNaph**: ^{1}H NMR (400 MHz, $CDCl_3$) δ 8.66 (ddd, *J* = 20.8, 7.9, 1.2 Hz, 2H), 8.50 (d, *J* = 7.6 Hz, 1H), 7.92 (d, *J* = 7.6 Hz, 1H), 7.81 (dd, *J* = 8.4, 7.3 Hz, 1H), 7.53 – 7.50 (m, 2H), 7.34 (dd, *J* = 8.4, 6.8 Hz, 2H), 7.27 3 (m, 1H), 6.56 (d, *J* = 7.2 Hz, 1H), 3.74 (s, 1H), 2.02 (d, *J* = 7.1 Hz, 3H).

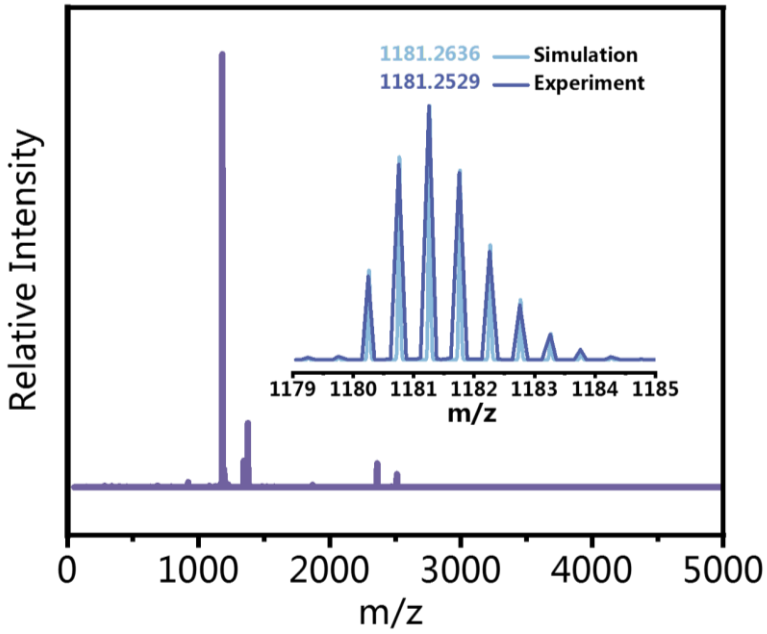

Figure S1. High resolution mass spectrometry of *R*-$PtAu_2$ cluster **1a**.

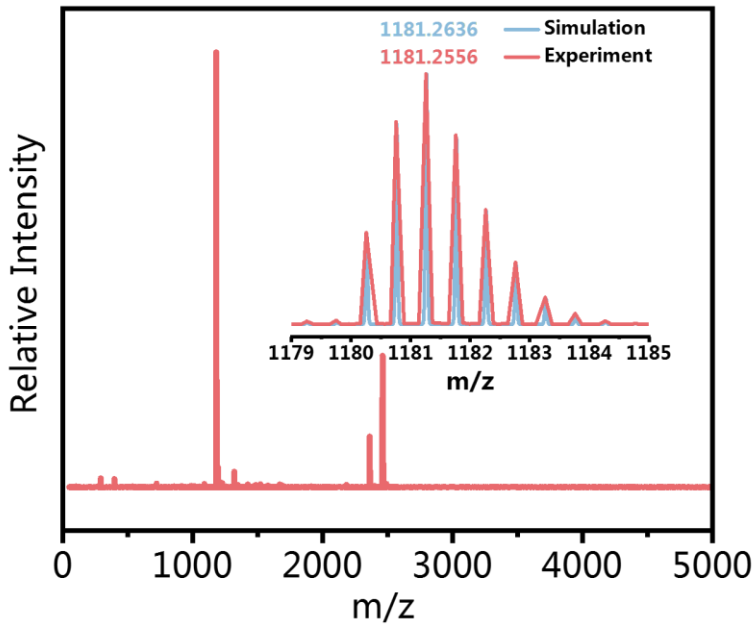

Figure S2. High resolution mass spectrometry of *S*-$PtAu_2$ cluster **1b**.

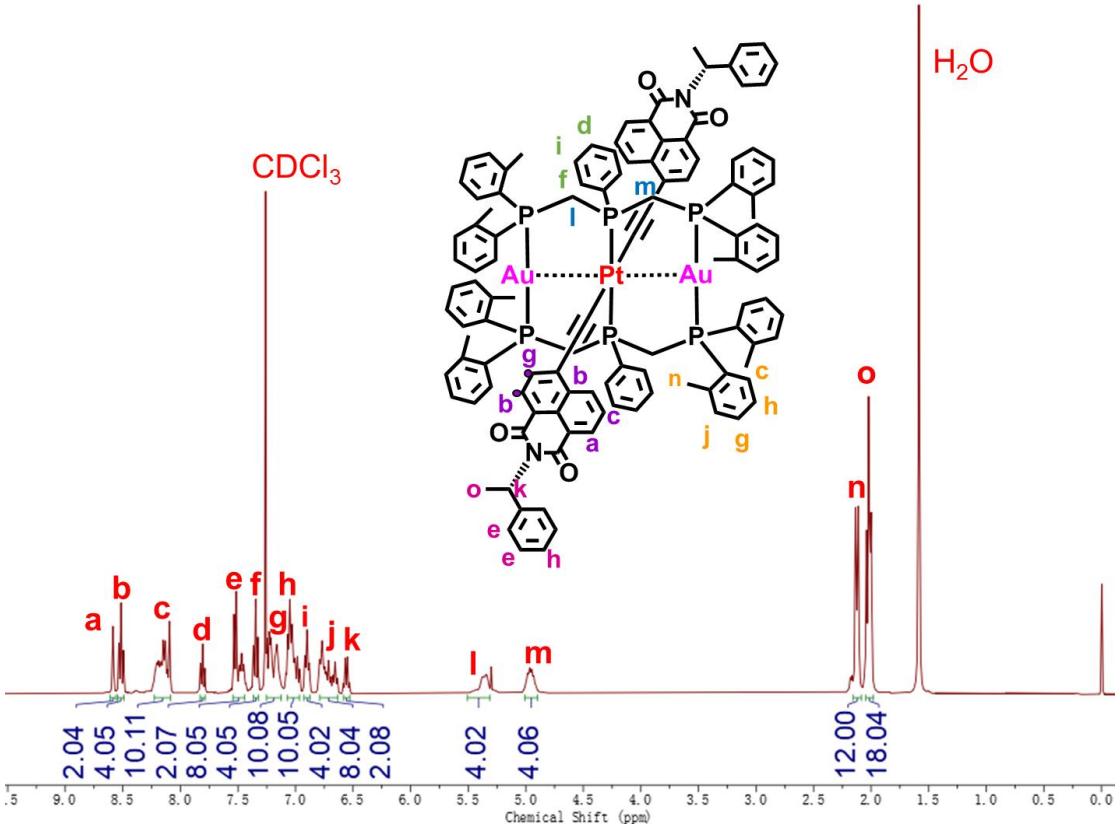

Figure S3. The ^{1}H NMR spectrum of *R*-PtAu$_2$ cluster **1a**, measured in $CDCl_3$.

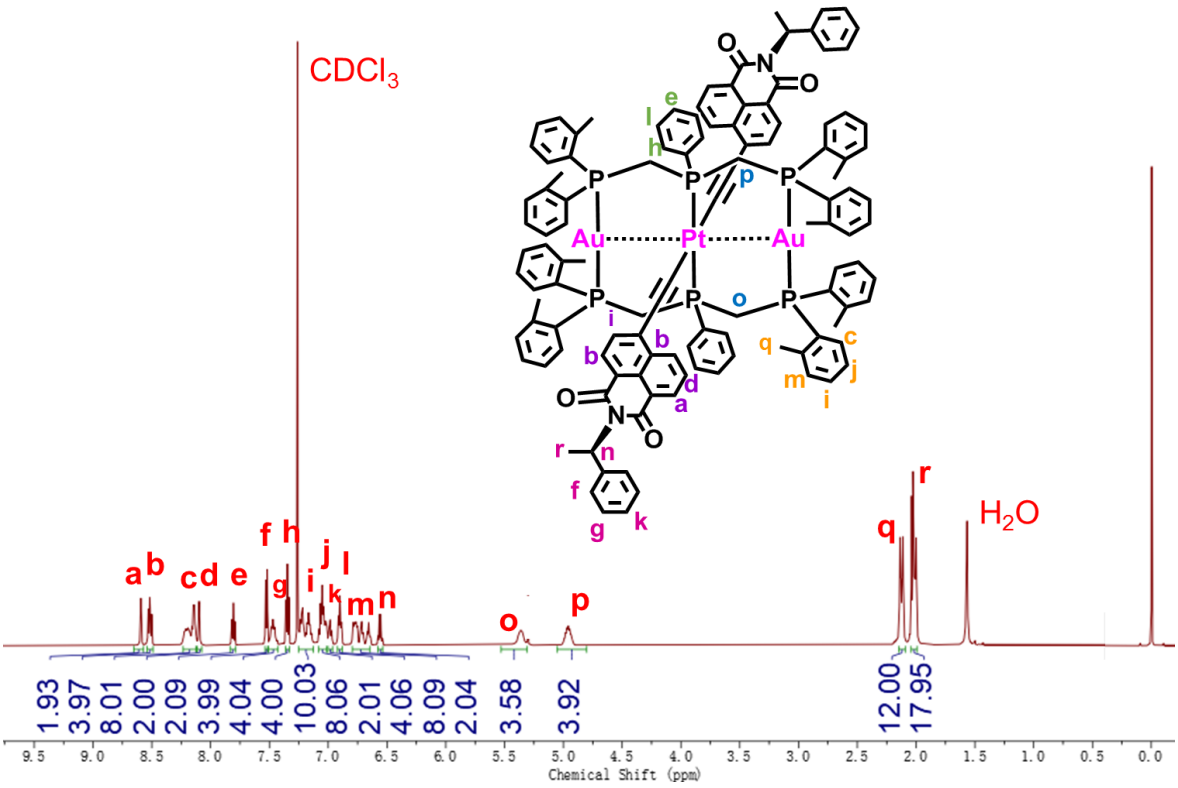

Figure S4. The ^{1}H NMR spectrum of *S*-PtAu$_2$ cluster **1b**, measured in $CDCl_3$.

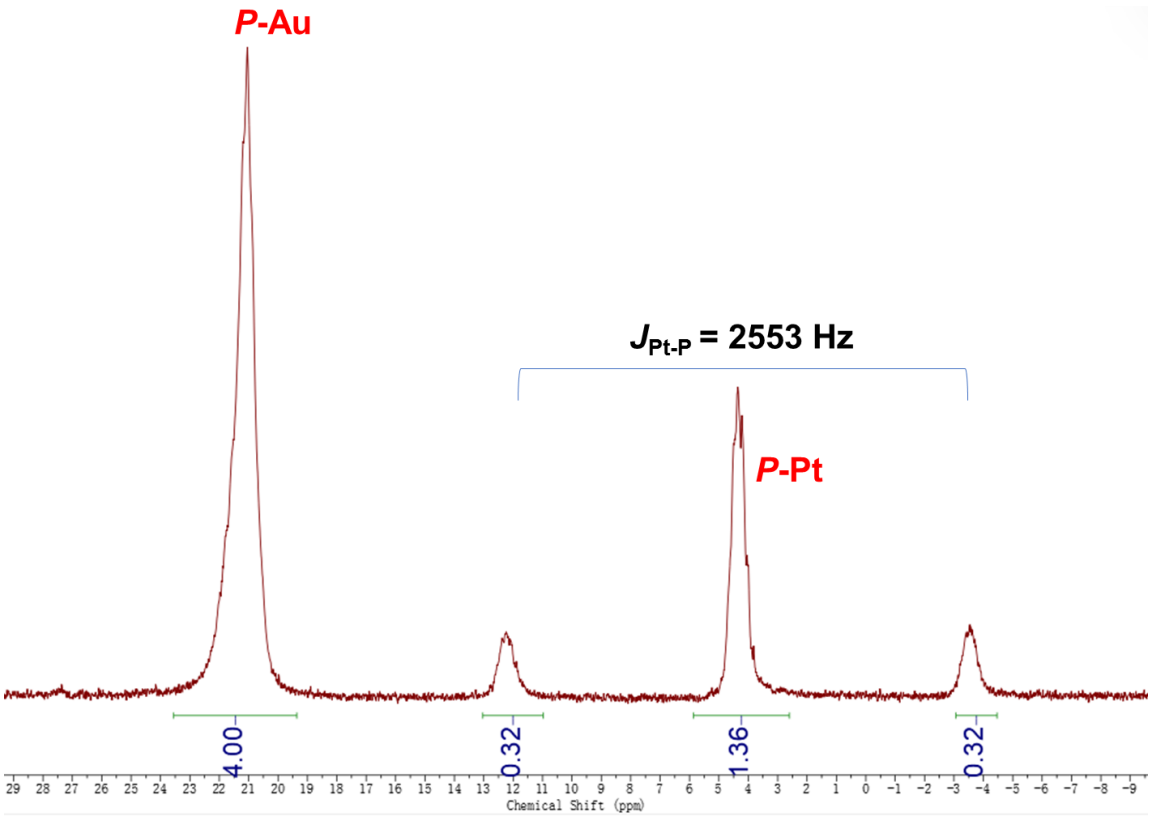

Figure S5. The ^{31}P NMR spectrum of *R*-PtAu$_2$ cluster **1a**, measured in CDCl$_3$.

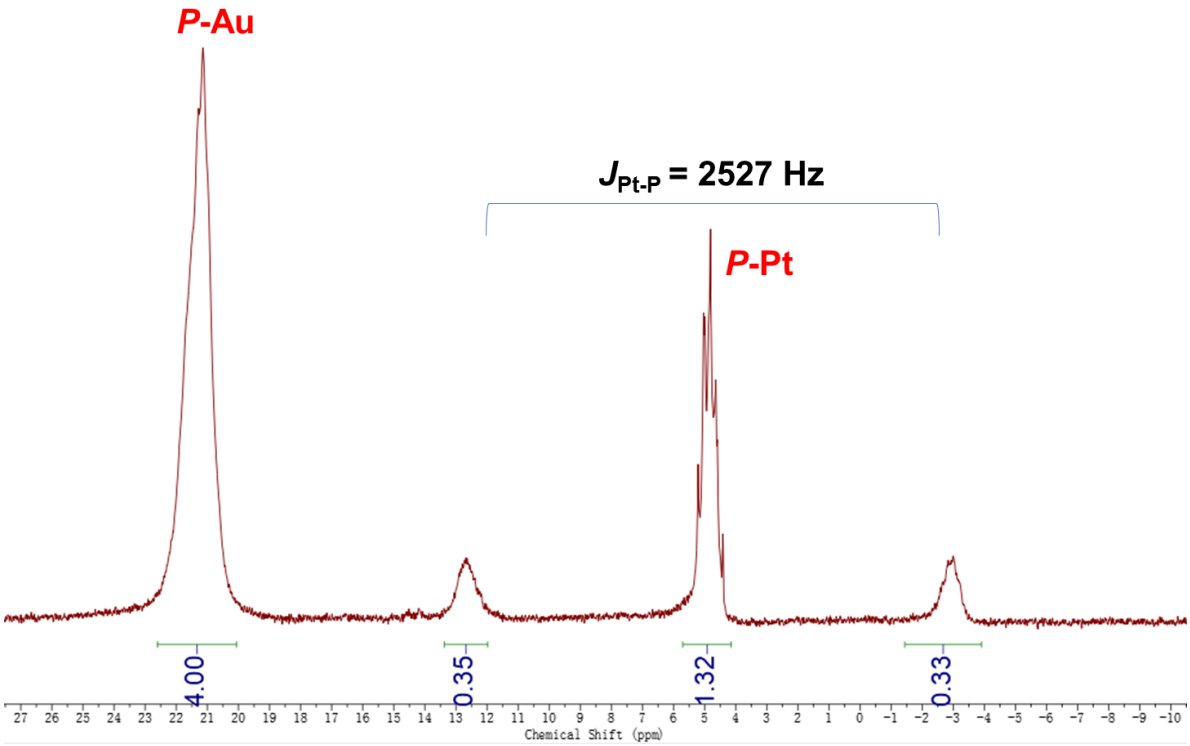

Figure S6. The ^{31}P NMR spectrum of *S*-PtAu$_2$ cluster **1b**, measured in CDCl$_3$.

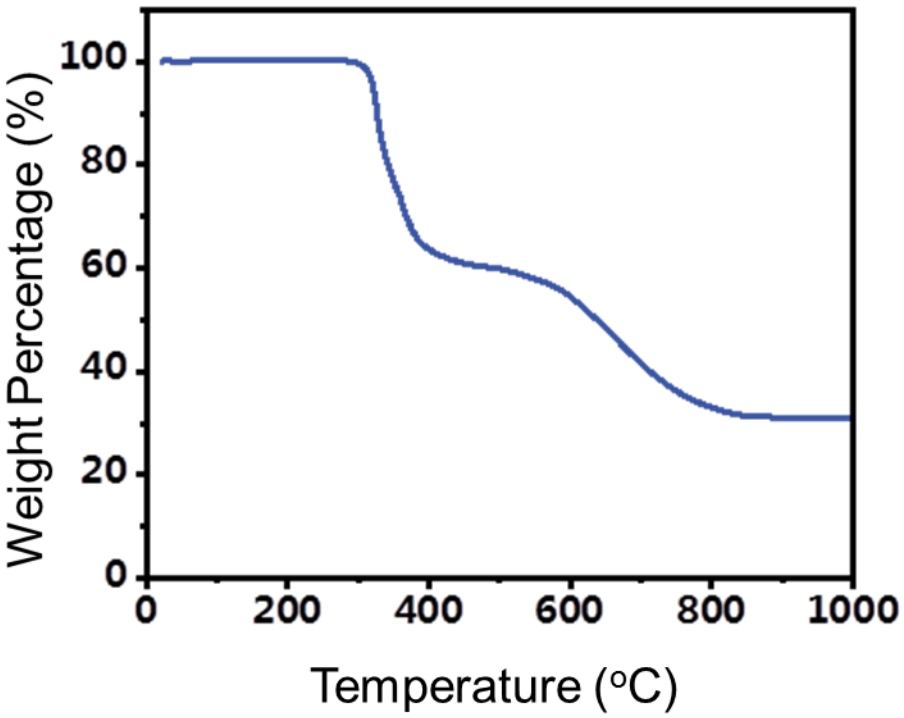

Figure S7. The plot of thermogravimetric analysis of *R*-$PtAu_2$ cluster **1a**.

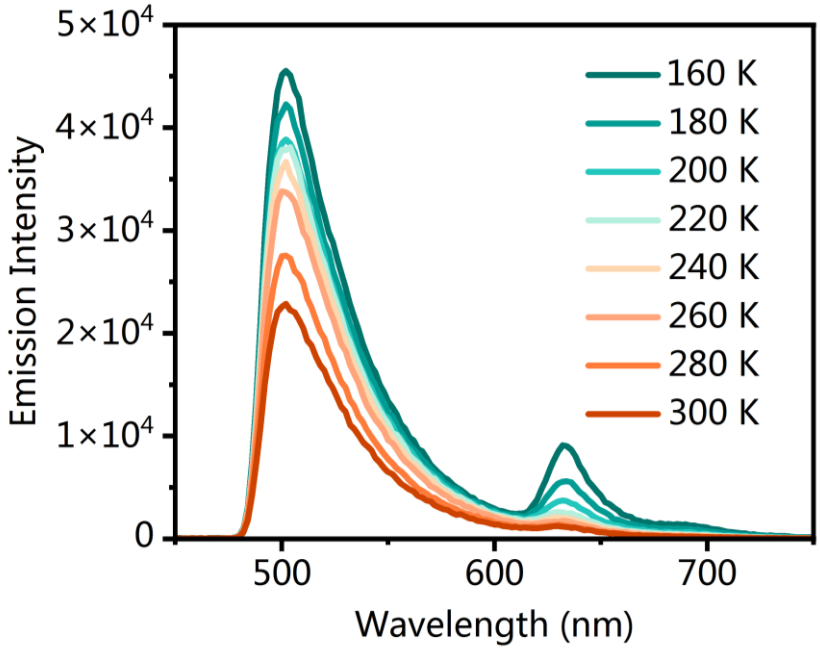

Figure S8. Variable-temperature emission spectra of mononuclear *R*-Pt complex precursor in CH_2Cl_2 at temperature range of 160–300 K.

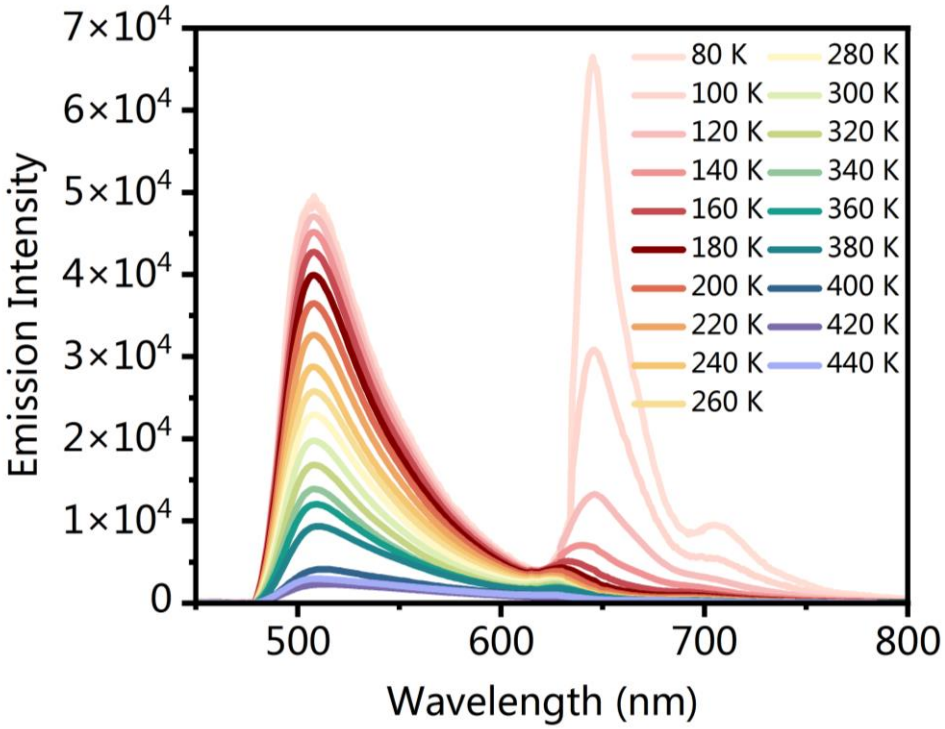

Figure S9. Variable-temperature emission spectra of mononuclear *R*-Pt complex precursor in solid state at temperature range of 80–440 K.

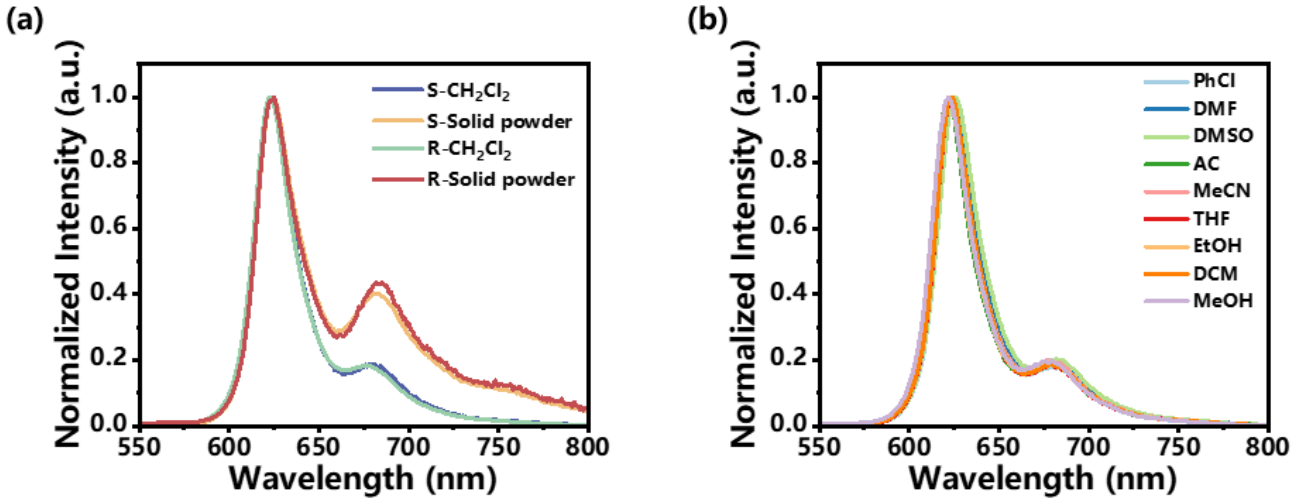

Figure S10. (a) The normalized emission spectra of *R*- and *S*-$PtAu_2$ clusters **1a** and **1b** and in CH_2Cl_2 and solid state. (b) The normalized emission spectra of *R*-$PtAu_2$ cluster **1a** in different solutions.

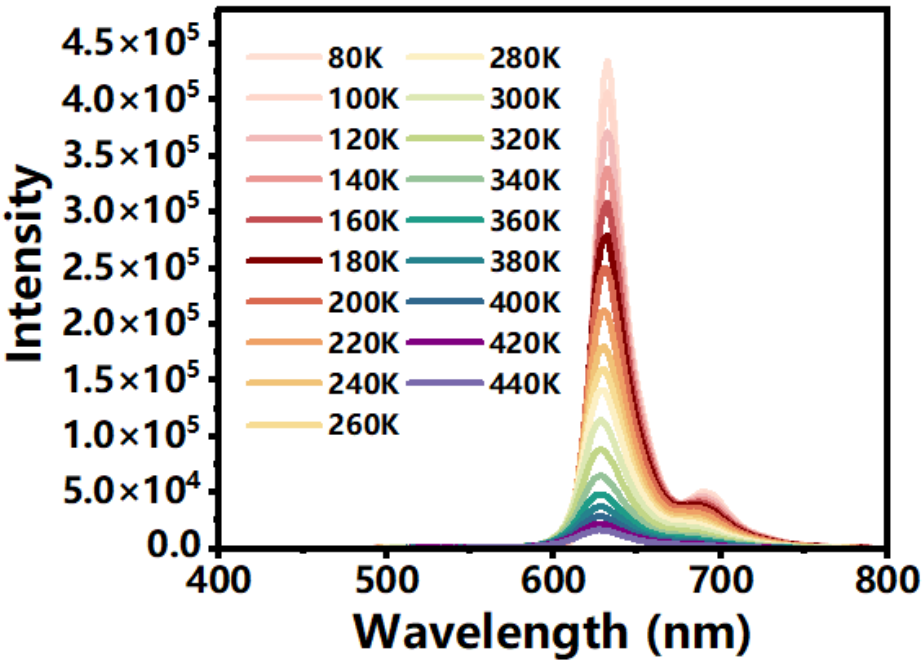

Figure S11. Variable-temperature emission spectra of *R*-$PtAu_2$ cluster **1a** in solid state at temperature range of 80–440 K.

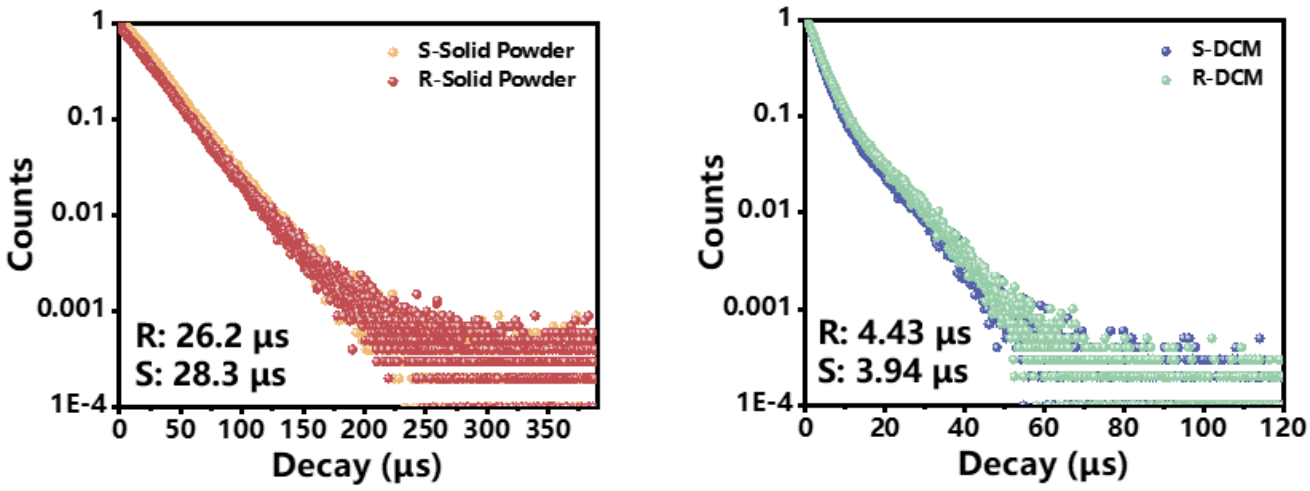

Figure S12. Decay curves of *R*- and *S*-$PtAu_2$ clusters **1a** and **1b** in solid state (a) and CH_2Cl_2 solutions (b).

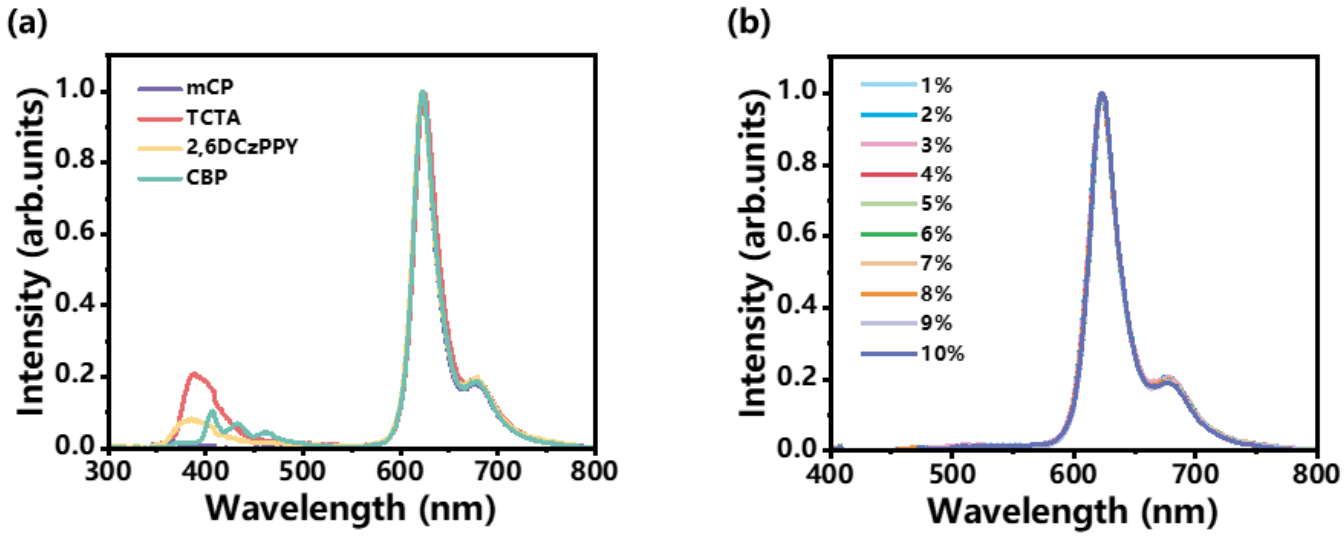

Figure S13. (a) Normalized emission spectra of *R*-$PtAu_2$ cluster **1a** in doping films. (b) Normalized emission spectra of *R*-$PtAu_2$ cluster **1a** in mCp doping films with different doping percentages.

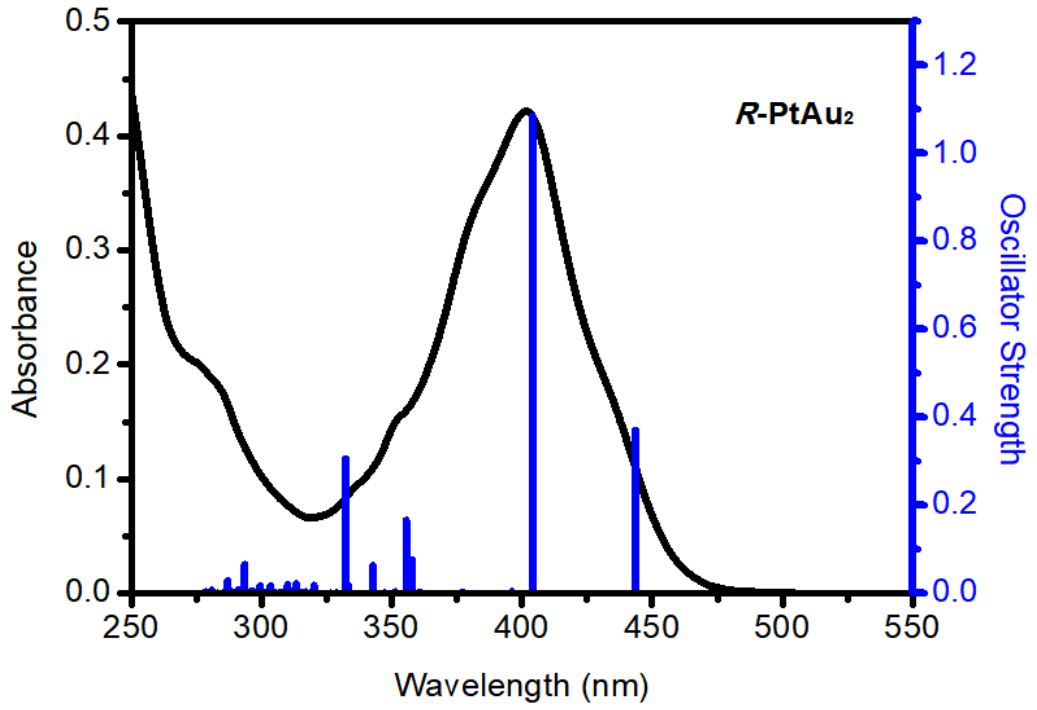

Figure S14. The calculated (blue vertical bars) and measured (black line) absorption spectra of *R*-$PtAu_2$ cluster **1a** in CH_2Cl_2 solution at ambient temperature calculated by TD-DFT method at the PBE1PBE level.

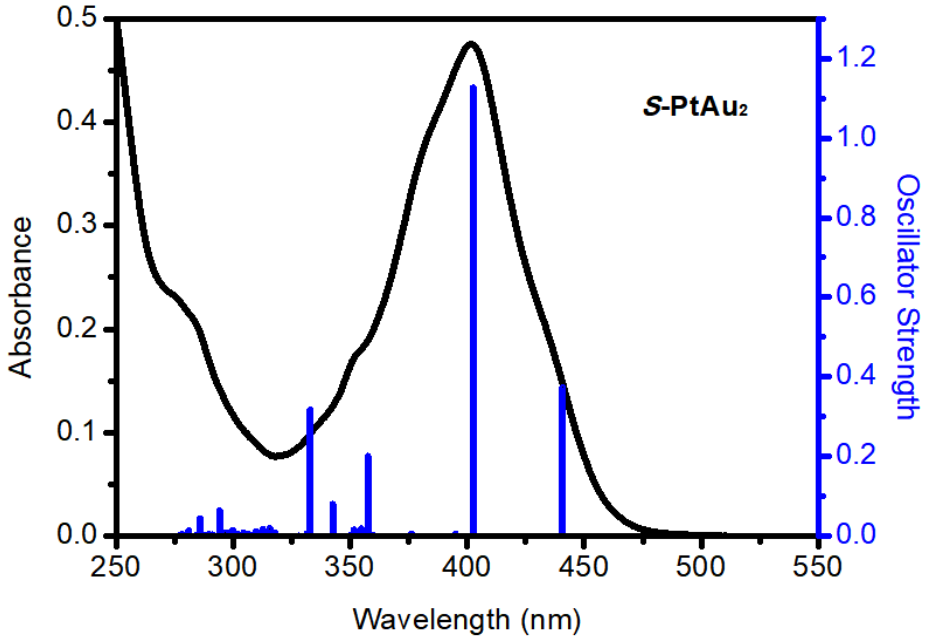

Figure S15. The calculated (blue vertical bars) and measured (black line) absorption spectra of *S*-$PtAu_2$ cluster **1b** in CH_2Cl_2 solution at ambient temperature calculated by TD-DFT method at the PBE1PBE level.

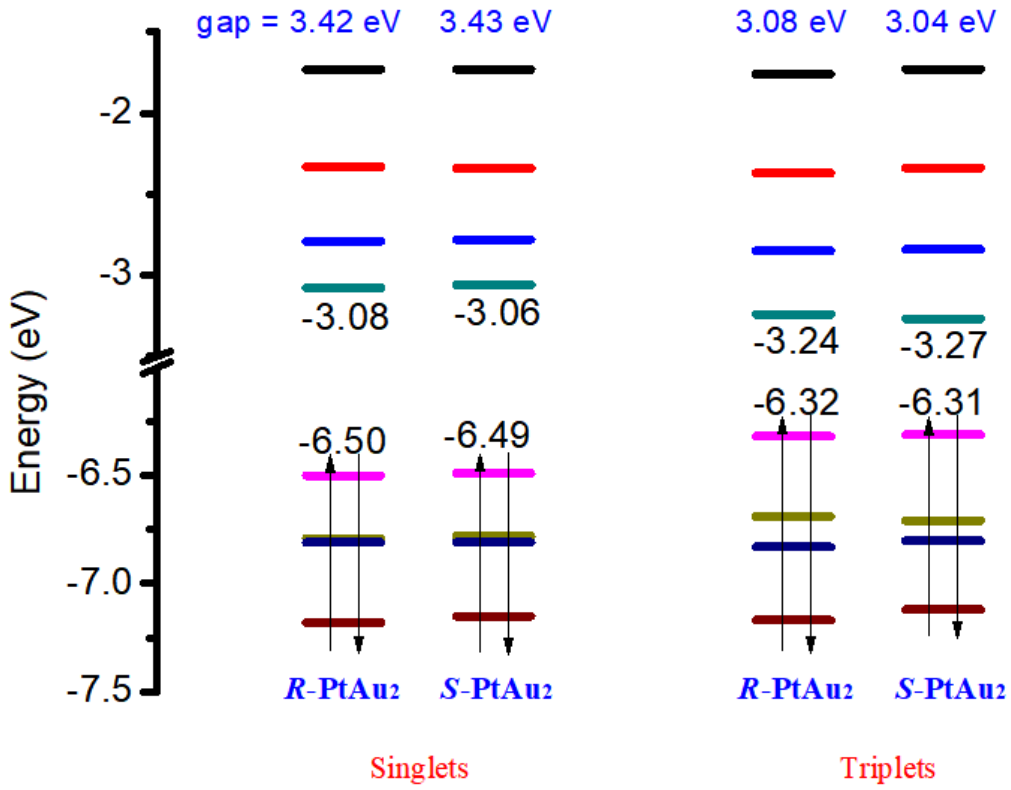

Figure S16. Plots of energy level of frontier orbitals in the lowest-energy singlet and triplet states for $PtAu_2$ clusters **1a** (*R*-$PtAu_2$) and **1b** (*S*-$PtAu_2$) in the CH_2Cl_2 solutions by TD-DFT method at the PBE1PBE level.

Table S1. Crystallographic Data of *R*/*S*-$PtAu_2$ Clusters **1a**·$2CHCl_3$ and **1b**·$3/2C_2H_4Cl_2$·$1/2CH_2Cl_2$.

	1a·$2CHCl_3$	**1b**·$3/2C_2H_4Cl_2$·$1/2CH_2Cl_2$
empirical formula	$C_{118}H_{102}Au_2Cl_8N_2O_{12}P_6Pt$	$C_{119.5}H_{109}Au_2Cl_6N_2O_{12}P_6Pt$
formula weight	2790.46	2752.64
crystal system	monoclinic	triclinic
space group	$P/2_1$	$P1$
a (Å)	15.0171(2)	15.2788 (1)
b (Å)	19.1160(2)	15.8413 (1)
c (Å)	24.6819(3)	25.2877 (2)
α (deg)		80.214 (1)
β (deg)	106.2340(10)	88.828 (1)
γ (deg)		77.078 (1)
V (Å^3)	6802.85(15)	5877.75 (8)
Z	2	1
ρ_{calcd} (g cm^{-3})	1.367	1.555
μ (mm^{-1})	3.455	6.313
radiation (λ, Å)	0.71073	1.3405
temperature (K)	100(2)	100
GOF	1.053	1.088
R1 (F_o)[a]	0.0548	0.0683
wR2 (F_o^2)[b]	0.1321	0.1950

[a] $R1 = \Sigma|F_o - F_c|/\Sigma F_o$. [b] $wR2 = \Sigma[w(F_o^2 - F_c^2)^2]/\Sigma[w(F_o)^2)]^{1/2}$

Table S2. The Absorption Transitions for *R*-$PtAu_2$ Cluster **1a** in the CH_2Cl_2 Solution Calculated by TD-DFT Method at the PBE1PBE Level.

state	*E*, nm (eV)	O.S.	transition (contrib.)	hole	electron	assignment
				Pt / Au / dTolmp / C≡CNaph-*R* (%)		
S1	444 (2.80)	0.3700	HOMO→LUMO (94%)	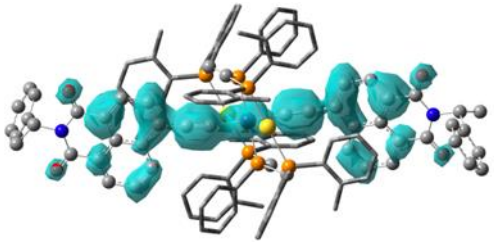 13.77/0.37/1.22/84.63	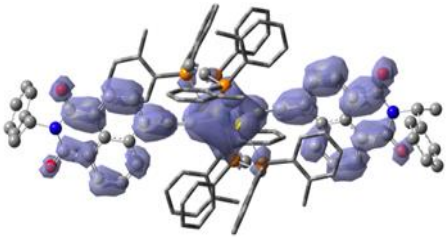 9.69/8.19/15.82/66.30	^{1}IL/^{1}LLCT/^{1}MC
S_2	404 (3.07)	1.0851	H-1→LUMO (92%)	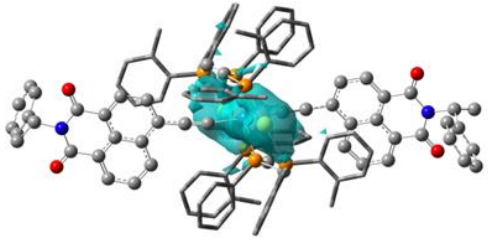 35.18/34.64/28.56/1.62	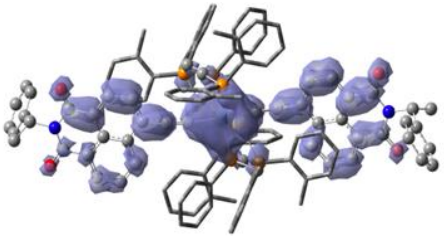 11.36/10.15/20.25/58.24	^{1}MLCT/^{1}MC
S_7	356 (3.49)	0.1660	HOMO→L+2 (41%) H-2→L+1 (29%) H-7→LUMO (17%)	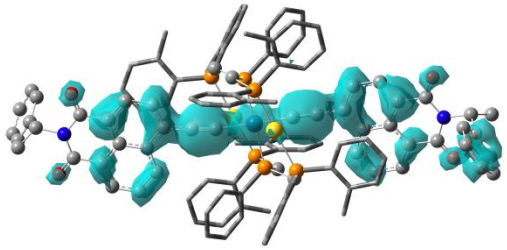 10.49/1.35/3.32/84.84	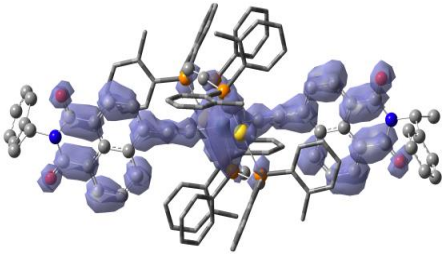 6.66/9.68/18.59/65.07	^{1}IL/^{1}LLCT/^{1}MC

S_{12}	332 (3.73)	0.3055	H-1→L+2 (87%)	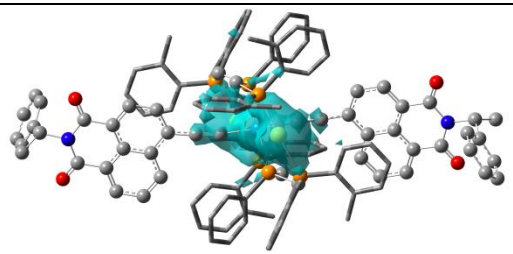	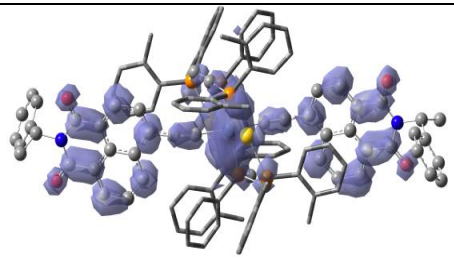	^{1}MLCT/^{1}IL /^{1}MC
				34.07/34.54/28.13/3.26	6.49/13.19/28.52/51.79	

Table S3. The Absorption Transitions for *S*-$PtAu_2$ Cluster **1b** in the CH_2Cl_2 Solution Calculated by TD-DFT Method at the PBE1PBE Level.

state	*E*, nm (eV)	O.S.	transition (contrib.)	hole	electron	assignment
				Pt / Au / dTolmp / C≡CNaph-*S* (%)		
S_1	441 (2.81)	0.3730	HOMO→LUMO (94%)	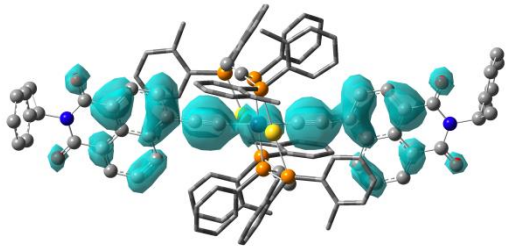	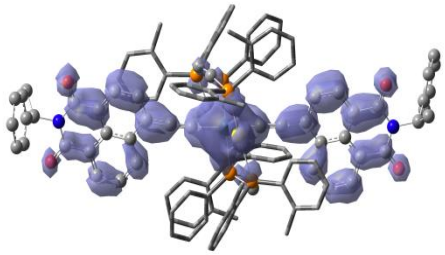	^{1}IL/^{1}LLCT/^{1}MC
				13.93/0.12/1.23/84.72	9.17/9.12/16.15/65.56	
S_2	403 (3.08)	1.1262	H-1→LUMO (94%)	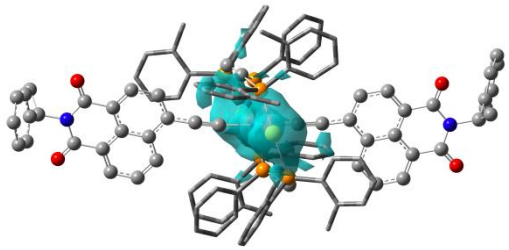	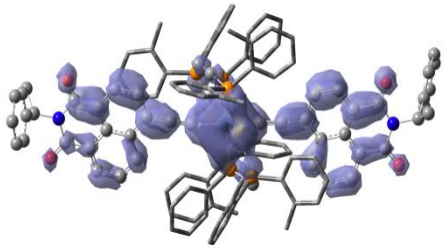	^{1}MLCT/^{1}MC /^{1}IL

				34.94/34.70/28.73/1.64	11.04/11.22/21.03/56.71	
S_6	358 (3.47)	0.2009	HOMO→L+2 (56%) H-2→L+1 (25%) H-7→LUMO (12%)	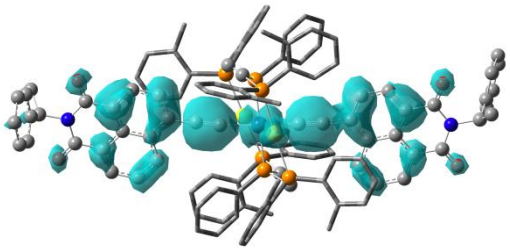	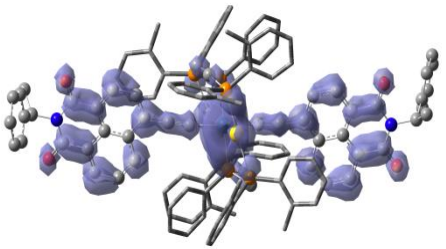	^{1}IL/^{1}LLCT/^{1}MC
				10.93/1.50/2.79/84.79	7.88/11.67/23.16/57.29	
S_{11}	333 (3.72)	0.3175	H-1→L+2 (92%)	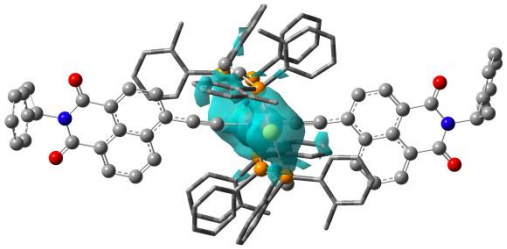	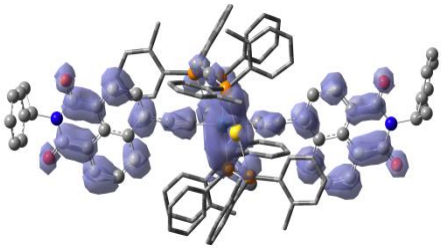	^{1}MLCT/^{1}IL/ ^{1}MC
				34.45/35.19/28.53/1.82	6.88/12.59/27.88/52.65	

Table S4. The Emission Transitions for *R*-$PtAu_2$ Cluster **1a** in the CH_2Cl_2 Solution Calculated by TD-DFT Method at the PBE1PBE Level.

state	*E*, nm (eV)	O.S.	transition (contrib.)	hole	electron	assignment
				Pt / Au / dTolmp / C≡CNaph-*R* (%)		
T_1	646 (1.92)	0.0000	HOMO→LUMO (66%) H-1→L+1 (25%)	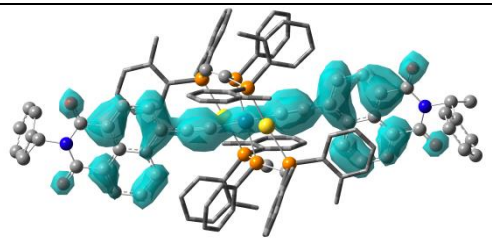 5.41/0.14/1.03/93.42	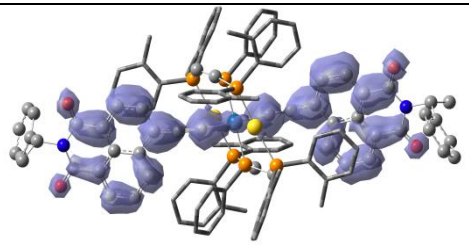 4.86/1.93/4.18/89.03	^{3}IL

Table S5. The Emission Transitions for *S*-$PtAu_2$ Cluster **1b** in the CH_2Cl_2 Solution Calculated by TD-DFT Method at the PBE1PBE Level.

state	*E*, nm (eV)	O.S.	transition (contrib.)	hole	electron	assignment
				Pt / Au / dTolmp / C≡CNaph-*S* (%)		
T_1	651 (1.91)	0.0000	HOMO→LUMO (76%) H-1→LUMO (10%)	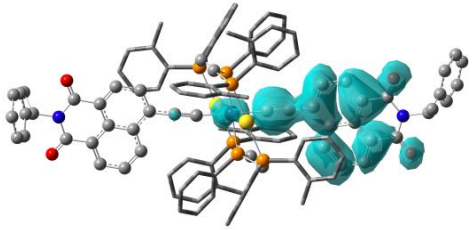 3.32/0.63/1.21/94.84	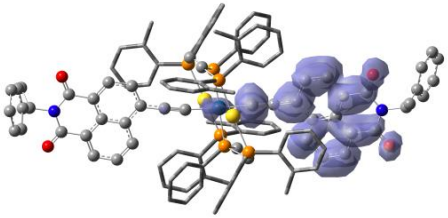 3.17/1.20/2.66/92.97	^{3}IL